Optical Properties, Thermochromism, and Crystal Structures of the Dimorphs of 2-Iodoanilinium Picrate

Masashi TANAKA,* Hiroaki MATSUI,† Jun-ichi MIZOGUCHI,†† and Setsuo KASHINO††
Department of Natural Science Informatics, School of Informatics and Sciences, Nagoya University, Chikusa-ku, Nagoya 464-01
† Department of Chemistry, Faculty of Science, Nagoya University, Chikusa-ku, Nagoya 464-01
†† Department of Chemistry, Faculty of Science, Okayama University, Tsushima, Okayama 700

(Received January 13, 1994)

The crystals of 2-iodoanilinium picrate have three polymorphic forms. The crystal structures of the monoclinic form (form **I**) and the triclinic form (form **II**) have been determined by the X-ray diffraction method. The crystals of the third form (form **III**) are unstable. In forms **I** and **II**, 2-iodoanilinium cation and picrate anion form a nearly planar pair of these ions with similar geometry of N–H···O hydrogen bond. In form **I** the pairs related by a translation are stacked to form the segregated columns, in which the same kinds of ions are stacked with each other, while in form **II** the anions and cations are alternately stacked to form the continuous columns. The thermochromism of these crystals was studied by measuring the polarized visible and IR absorption spectra and the differential scanning calorimetry.

It is well known that picric acid forms salts or charge-transfer (CT) complexes with many organic compounds.[1] That is, picrate salts are formed with aromatic and aliphatic amines,[2] while π CT complexes of picric acid are formed with aromatic hydrocarbons.[3] However, a few crystals of picrate salts with aromatic amines showed the thermochromism and changed to CT complexes upon heating.[2] In this paper, we report the polarized visible and IR absorption spectra and the X-ray crystal structures of the salts of 2-iodoaniline with picric acid. Furthermore, we discuss the mechanism of the thermochromism based on the spectral data and the crystal structures.

Experimental

Optical Properties and Thermochromism of the Crystals of Picric Acid and 2-Iodoaniline Complexes. Picric acid (Tokyo Kasei Co.) and 2-iodoaniline (Aldrich Chemical Co.) were used without furthermore purification. Crystals were obtained by slow evaporation of approximately equimolar solutions of the components. The yellow needle-shaped crystals (form **I**) were obtained from methanol solution, and the dark green plate-like crystals (form **II**) and the red plate-like crystals (form **III**) were obtained from benzene solution. The crystals of form **I** and **II** were stable but the crystals of form **III** changed to the yellow ones in a day. The thermal treatment of the crystals was made by heating at about 60 °C for a few min in air. Thermal analyses were carried out using a Shimadzu DSC-50 (a TGA-50) at a heating rate of 10 °C min^{-1} under N_2 gas. The polarized IR absorption spectra of the single crystal were recorded using a JASCO FTIR VALOR-III. The visible absorption spectra of the single crystal were taken using a polarized absorption microspectrophotometer made in our laboratory.[4]

X-Ray Structure Analysis. Experimental details and crystal data are listed in Table 1. Intensity data for forms **I** and **II** were measured on a Rigaku AFC-5R four-circle diffractometer with graphite monochromated Mo $K\alpha$ radiation (λ=0.71073 Å, 40 kV, 200 mA). The fluctuations

Table 1. Experimental Details and Crystal Data

	Form **I**	Form **II**
Chemical formula	$C_{12}H_9N_4O_7$ I	$C_{12}H_9N_4O_7$ I
Formula weight	448.13	448.13
Crystal color	Yellow	Green
Crystal habits	Prismatic	Plate
Crystal size/mm	0.10×0.08×0.50	0.30×0.18×0.55
No. of reflections used for unit cell determination		
(2θ range/°)	25 (21—22)	25 (18—20)
Crystal system	Monoclinic	Triclinic
Space group	$P2_1/n$	$P\bar{1}$
a/Å	14.492(2)	7.323(2)
b/Å	4.3733(8)	8.245(1)
c/Å	24.153(5)	13.656(2)
α/°		75.71(1)
β/°	98.81(2)	74.05(2)
γ/°		75.64(2)
V/Å^3	1512.6(5)	753.7(6)
Z	4	2
D_X/Mg m^{-3}	1.968	1.974
$F(000)$	872	436
μ(Mo $K\alpha$)/mm^{-1}	2.14	2.14
T/K	293	298
Scan type	ω	ω–2θ
Scan width ω/°	1.21+0.30 tanθ	1.21+0.30 tan θ
Scan speed in ω/°min^{-1}	6	6
$2\theta_{max}$/°	50.0	52.0
Range of h,k,l	$0\leq h\leq 17$	$0\leq h\leq 9$
	$0\leq k\leq 5$	$-10\leq k\leq 10$
	$-28\leq l\leq 28$	$-16\leq l\leq 16$
Fluctuation of standard reflections/%	1.9	1.0
R_{int}	0.021	0.008
No. of reflections used	1685	2548
	$I_0>3.0\sigma(I_0)$	$I_0>3.0\sigma(I_0)$
No. of parameters	253	253
R/wR	0.040/0.030	0.022/0.023
S	1.38	1.53
$(\Delta/\sigma)_{max}$	0.18	0.49
$\Delta\rho_{max}$/eÅ^{-3}	0.77	0.38
$\Delta\rho_{min}$/eÅ^{-3}	−1.00	−0.36

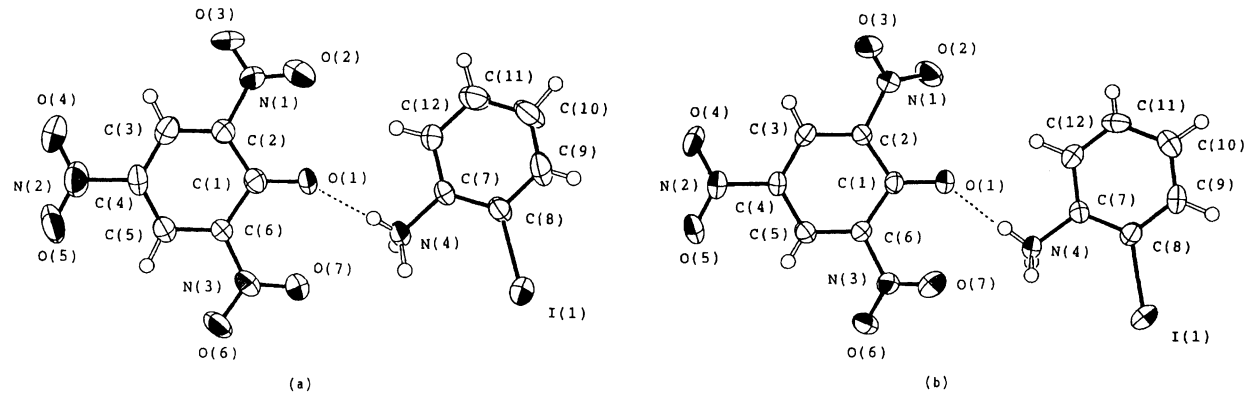

Fig. 1. The thermal ellipsoids drawn at 50% probability, and atomic numbering of non-H atoms. A hydrogen bond between the cation and the anion is shown by a broken line. (a) Form **I**, and (b) Form **II**.

Table 2. Fractional Atomic Coordinates and Equivalent Thermal Parameters B_{eq} with Their esd's in Parentheses

$$B_{eq} = (8\pi^2/3)\sum_i\sum_j U_{ij}a_i^*a_j^*\boldsymbol{a}_i\cdot\boldsymbol{a}_j.$$

Atom	x	y	z	B_{eq}/Å^2
Form **I**				
I(1)	0.39194(3)	−0.0678(1)	0.25573(2)	4.10(2)
O(1)	0.6839(3)	0.738(1)	0.3675(2)	3.3(2)
O(2)	0.6650(4)	1.039(2)	0.4590(3)	10.3(5)
O(3)	0.7708(6)	1.238(3)	0.5026(4)	19.7(9)
O(4)	1.0712(4)	1.333(2)	0.4496(3)	7.4(4)
O(5)	1.0994(3)	1.105(2)	0.3738(2)	7.4(4)
O(6)	0.8795(3)	0.453(1)	0.2722(2)	4.3(2)
O(7)	0.7493(3)	0.345(1)	0.2990(2)	4.1(3)
N(1)	0.7423(5)	1.103(2)	0.4648(3)	4.6(3)
N(2)	1.0496(4)	1.164(2)	0.4089(3)	5.1(4)
N(3)	0.8213(4)	0.494(1)	0.3036(2)	3.0(3)
N(4)	0.5733(4)	0.246(2)	0.3333(3)	3.1(3)
C(1)	0.7697(5)	0.810(2)	0.3801(3)	2.7(3)
C(2)	0.8050(5)	1.006(2)	0.4261(3)	3.0(4)
C(3)	0.8938(5)	1.114(2)	0.4363(3)	3.4(4)
C(4)	0.9554(4)	1.027(2)	0.4011(3)	3.3(4)
C(5)	0.9311(5)	0.832(2)	0.3579(3)	2.9(4)
C(6)	0.8412(4)	0.714(2)	0.3318(3)	2.5(3)
C(7)	0.4868(4)	0.292(2)	0.3574(3)	2.5(3)
C(8)	0.4033(4)	0.162(2)	0.3316(3)	3.1(3)
C(9)	0.3252(5)	0.202(2)	0.3579(4)	4.1(4)
C(10)	0.3286(5)	0.369(2)	0.4056(3)	4.8(5)
C(11)	0.4113(5)	0.503(2)	0.4295(3)	4.4(5)
C(12)	0.4914(5)	0.462(2)	0.4057(3)	3.4(4)

Table 2. (Continued)

Atom	x	y	z	B_{eq}/Å^2
Form **II**				
I(1)	−0.20130(3)	0.07332(2)	0.88089(1)	4.27(1)
O(1)	0.2743(2)	0.0498(2)	0.4524(1)	3.2(1)
O(2)	0.4137(3)	−0.2043(2)	0.3415(2)	4.1(1)
O(3)	0.7055(3)	−0.1863(2)	0.2571(1)	4.0(1)
O(4)	0.7420(3)	0.3562(3)	0.0194(1)	4.7(2)
O(5)	0.6100(3)	0.5855(2)	0.0808(2)	5.0(2)
O(6)	0.1712(3)	0.5569(2)	0.4164(2)	4.6(1)
O(7)	0.2552(3)	0.3338(3)	0.5279(2)	4.8(2)
N(1)	0.5401(3)	−0.1215(2)	0.2967(2)	2.8(1)
N(2)	0.6396(3)	0.4308(3)	0.0885(2)	3.2(2)
N(3)	0.2534(3)	0.4092(3)	0.4389(2)	3.1(2)
N(4)	0.0217(4)	0.0787(3)	0.6367(2)	3.1(2)
C(1)	0.3674(3)	0.1354(3)	0.3735(2)	2.2(1)
C(2)	0.4958(3)	0.0626(3)	0.2886(2)	2.2(1)
C(3)	0.5857(3)	0.1559(3)	0.1973(2)	2.4(2)
C(4)	0.5511(3)	0.3302(3)	0.1849(2)	2.4(2)
C(5)	0.4390(3)	0.4116(3)	0.2644(2)	2.5(2)
C(6)	0.3567(3)	0.3170(3)	0.3555(2)	2.3(1)
C(7)	0.0231(3)	−0.0960(3)	0.6960(2)	2.3(1)
C(8)	−0.0715(3)	−0.1252(3)	0.7992(2)	2.6(2)
C(9)	−0.0771(4)	−0.2923(3)	0.8516(2)	3.3(2)
C(10)	0.0132(4)	−0.4252(3)	0.8002(2)	3.6(2)
C(11)	0.1099(4)	−0.3914(3)	0.6960(2)	3.2(2)
C(12)	0.1159(3)	−0.2305(3)	0.6453(2)	2.7(2)

of the intensities of three standard reflections were measured after every 97 reflections. The data were corrected for Lorentz and polarization effects. An absorption correction was applied based on azimuthal scans of three reflections. The transmission factors ranged from 0.89 to 1.00 for form **I**, and from 0.76 to 1.00 for form **II**. The structures of forms **I** and **II** were solved by directed methods (MITHRIL[5]) and the Patterson method, respectively. For both structures the non-H atoms were refined anisotropically and the H atoms isotropically by full matrix least-squares method: $\sum w(|F_o|-|F_c|)^2$ was minimized with $w=\sigma(F_o)^{-2}$. The atomic scattering factors were taken from International Tables for X-Ray Crystallography.[6] Calculations were performed by using the TEXSAN[7] at the X-Ray Laboratory of Okayama University.

Results and Discussion

Crystal and Molecular Structure. Final atomic parameters for the crystals of forms **I** and **II** are listed in Table 2.[8] The ORTEP drawing and the numbering of atoms are shown in Fig. 1, where the same numbering scheme is adopted for both forms. The bond lengths and angles are listed in Table 3. Projections of the crystal structures are shown in Fig. 2. The symmetry codes are given in Figs. 2 and 3. The 2-iodoanilinium cation

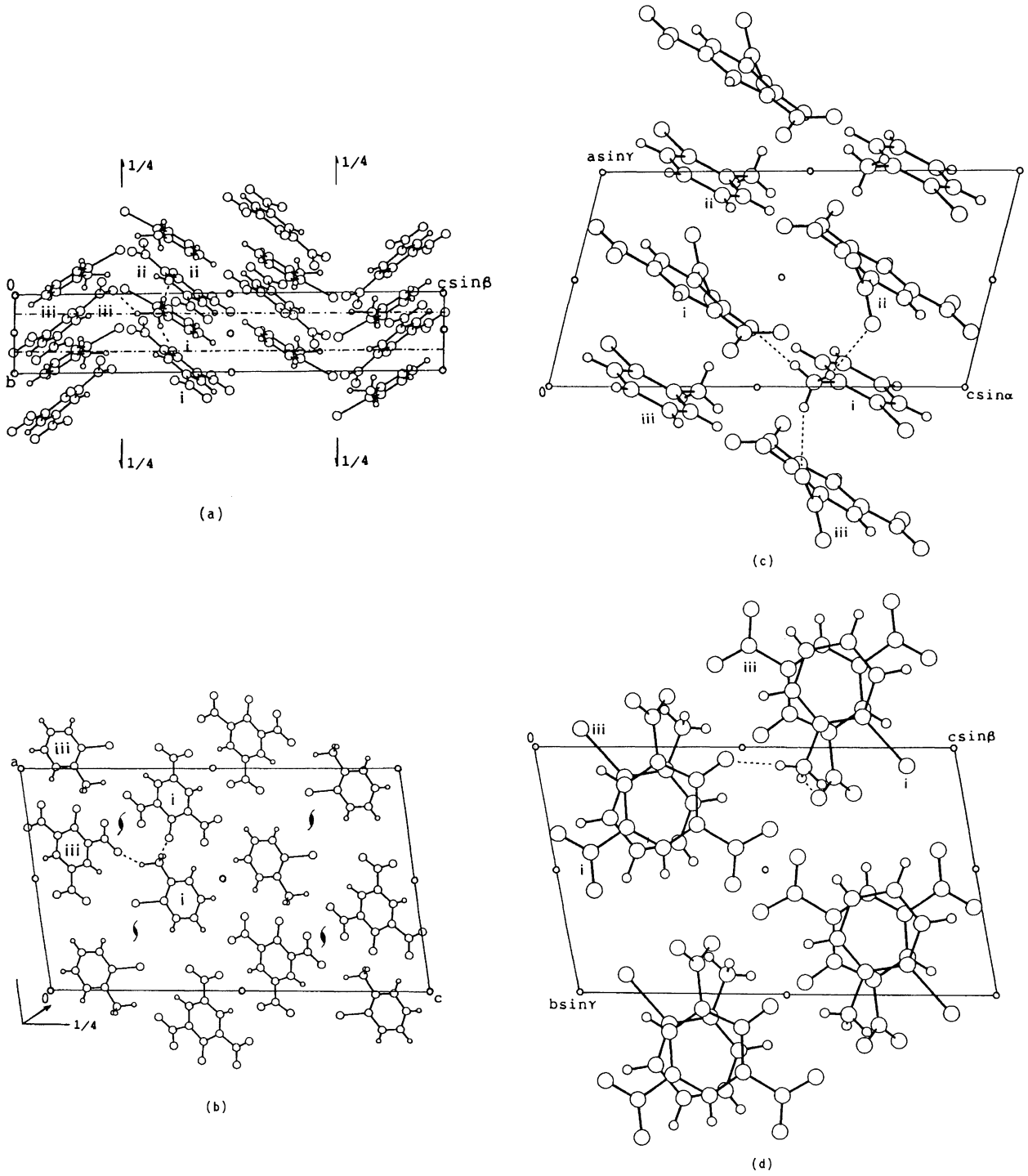

Fig. 2. Projections of the crystal structures. Hydrogen bonds are shown by broken lines. (a) Form **I** viewed down the a axis, (b) form **I** viewed down the b axis, (c) form **II** viewed down the b axis, and (d) form **II** viewed down the a axis. Symmetry codes: (i) x, y, z; (ii) x, $-1+y$, z; (iii) $3/2-x$, $-1/2+y$, $1/2-z$ for form **I**, and (i) x, y, z; (ii) $1-x$, $-y$, $1-z$; (iii) $-x$, $-y$, $1-z$ for form **II**.

and picrate anion chosen as an asymmetric unit form a hydrogen-bonded pair in both forms. The arrangement of the cation and anion in the pair of form **I** is similar to that in form **II**, as seen from Fig. 1. The geometries of the hydrogen bond are: N(4)···O(1) 2.733(8), H(3N)···O(1) 1.90(8) Å, and N(4)–H(3N)···O(1) 166(8)° for form **I**, and the corresponding geometries for form **II** are 2.708(3), 1.88(3), and 177(3) Å, respectively. In these two forms a similarity is also found in the arrangements of the pairs related by a translation, that is, the arrangement of the pairs along [1 1 0] for form **I** is similar to that along [1 1 $\bar{1}$] for form **II** as shown in Fig. 3.

In the crystal of form **I** the pairs of the ions related

Table 3. Bond Lengths (l/Å) and Angles (ϕ/°)

	Form **I**	Form **II**
2-Iodoanilinium cation		
I(1)–C(8)	2.076(7)	2.092(2)
N(4)–C(7)	1.474(8)	1.467(3)
C(7)–C(8)	1.394(9)	1.379(3)
C(7)–C(12)	1.376(9)	1.385(3)
C(8)–C(9)	1.391(9)	1.391(3)
C(9)–C(10)	1.36(1)	1.377(4)
C(10)–C(11)	1.38(1)	1.397(4)
C(11)–C(12)	1.384(9)	1.342(4)
N(4)–C(7)–C(8)	120.0(6)	120.6(2)
N(4)–C(7)–C(12)	118.4(6)	118.5(2)
C(8)–C(7)–C(12)	121.6(6)	120.8(2)
I(1)–C(8)–C(7)	122.6(5)	122.1(2)
I(1)–C(8)–C(9)	120.2(6)	118.7(2)
C(7)–C(8)–C(9)	117.2(7)	119.1(2)
C(8)–C(9)–C(10)	121.8(8)	119.7(2)
C(9)–C(10)–C(11)	120.0(7)	119.8(2)
C(10)–C(11)–C(12)	120.0(8)	120.7(2)
C(7)–C(12)–C(11)	119.2(7)	119.9(2)
Picrate anion		
O(1)–C(1)	1.274(7)	1.259(3)
O(2)–N(1)	1.143(7)	1.222(3)
O(3)–N(1)	1.111(8)	1.227(3)
O(4)–N(2)	1.232(8)	1.225(3)
O(5)–N(2)	1.221(8)	1.223(3)
O(6)–N(3)	1.230(6)	1.222(3)
O(7)–N(3)	1.221(6)	1.223(3)
N(1)–C(2)	1.463(8)	1.455(3)
N(2)–C(4)	1.475(9)	1.449(3)
N(3)–C(6)	1.445(8)	1.454(3)
C(1)–C(2)	1.432(9)	1.433(3)
C(1)–C(6)	1.441(8)	1.442(3)
C(2)–C(3)	1.356(9)	1.380(3)
C(3)–C(4)	1.378(9)	1.372(3)
C(4)–C(5)	1.353(9)	1.378(3)
C(5)–C(6)	1.387(9)	1.364(3)
O(2)–N(1)–O(3)	117.6(8)	123.1(2)
O(2)–N(1)–C(2)	123.0(7)	119.5(2)
O(3)–N(1)–C(2)	119.4(7)	117.4(2)
O(4)–N(2)–O(5)	125.1(7)	123.3(2)
O(4)–N(2)–C(4)	117.5(7)	118.3(2)
O(5)–N(2)–C(4)	117.3(7)	118.3(2)
O(6)–N(3)–O(7)	121.5(6)	123.8(2)
O(6)–N(3)–C(6)	118.8(6)	118.5(2)
O(7)–N(3)–C(6)	119.6(5)	117.7(2)
O(1)–C(1)–C(2)	123.6(6)	123.4(2)
O(1)–C(1)–C(6)	123.7(6)	125.1(2)
C(2)–C(1)–C(6)	112.6(6)	111.5(2)
N(1)–C(2)–C(1)	119.1(6)	119.6(2)
N(1)–C(2)–C(3)	116.5(7)	116.0(2)
C(1)–C(2)–C(3)	124.4(7)	124.4(2)
C(2)–C(3)–C(4)	118.6(7)	119.0(2)
N(2)–C(4)–C(3)	119.0(7)	119.8(2)
N(2)–C(4)–C(5)	118.8(7)	119.1(2)
C(3)–C(4)–C(5)	122.1(7)	121.0(2)
C(4)–C(5)–C(6)	119.3(7)	119.2(2)
N(3)–C(6)–C(1)	121.0(6)	119.2(2)
N(3)–C(6)–C(5)	116.4(6)	116.3(2)
C(1)–C(6)–C(5)	122.5(7)	124.5(2)

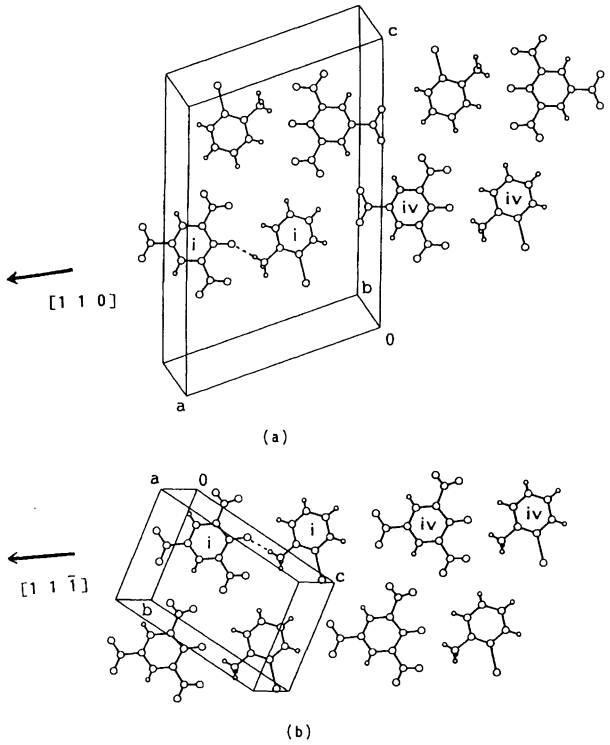

Fig. 3. Diagrams showing a similarity of the molecular arrangements in form **I** (a) and form **II** (b). Hydrogen bond between a pair of the cation and anion is shown by a broken line. Symmetry codes; (i) x, y, z; (iv) $-1+x$, $-1+y$, z for form **I**, and (i) x, y, z; (iv) $-1+x$, $-1+y$, $1+z$ for form **II**.

by a b translation are stacked to form the segregated columns as shown in Fig. 2(a) and (b). The views of the molecular overlapping in each column are shown in Fig. 4(a) for the cations and in Fig. 4(b) for the anions. The spacing between the benzene-ring planes of the stacking ions is 3.618 Å for the cations, and 3.405 Å for the anions. The shortest contact between the overlapping ions is 3.64(1) Å for C(9)···C(11) for the cations, and 3.39(1) Å for C(3)···C(6) for the anions. Between the adjacent columns there are two additional N–H···O hydrogen bonds: The anilinium cation (i) is linked to the picrate anions (ii) and (iii). The geometries of the hydrogen bonds are: N(4)···O(1) 2.792(9), H(1N)···O(1) 1.91(8) Å, N(4)–H(1N)···O(1) 168(7)°, and N(4)···O(6) 3.023(8), H(2N)···O(6) 2.18(8) Å, N(4)···H(2N)–O(6) 131(5)°, respectively.

In the crystal of form **II** the cation and anion are stacked along the a axis to form the continuous columns as shown in Fig. 2(c) and (d). The molecular overlapping in the column is shown in Fig. 4(c) and (d). The dihedral angle between the benzene-ring planes of the overlapping cation and anion is 6.6(1)°. The shortest intermolecular contact observed in the column is 3.360(3) Å between C(1) and C(7^{iii}). Two fairly weak N–H···O hydrogen bonds are formed between the anilinium N of the cation (i) and the O atoms of the nitro groups

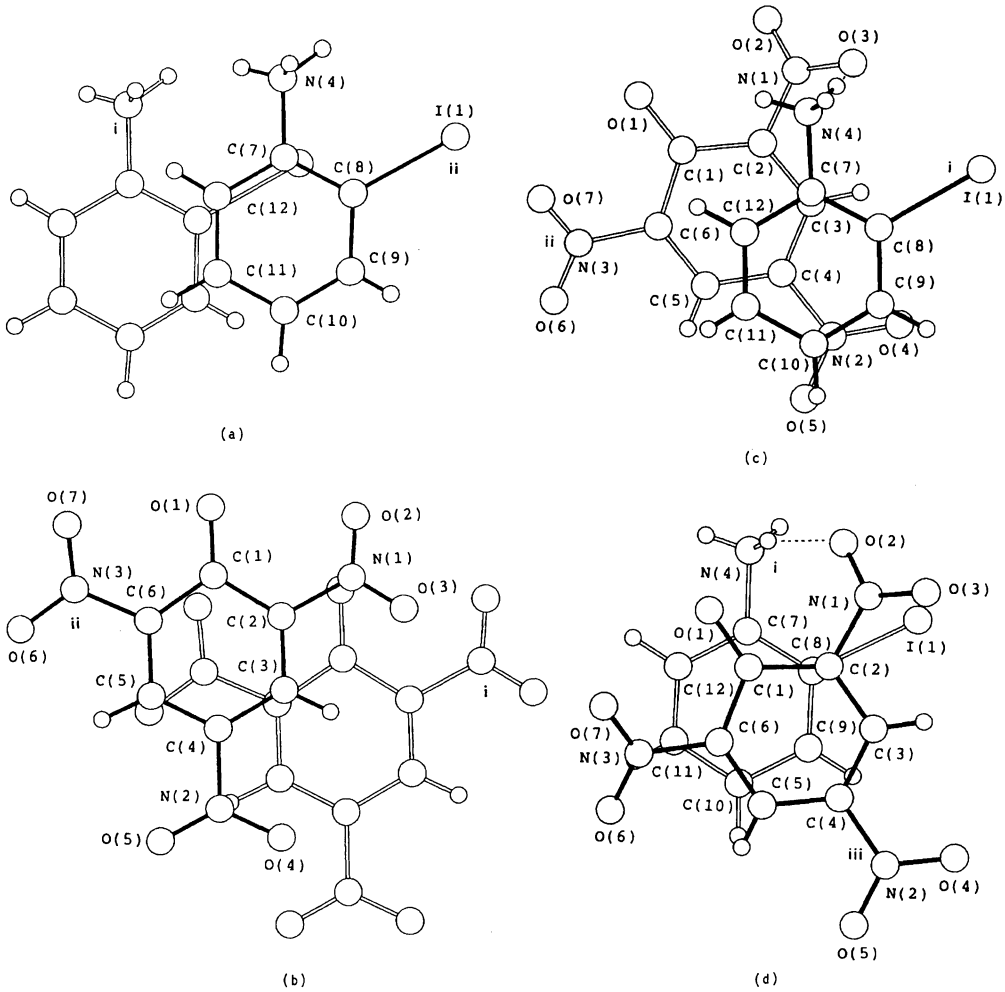

Fig. 4. Molecular overlapping (a) between the cations in form **I**, (b) between the anions in form **I**, (c) between the cation (i) and the anion (ii) in form **II**, and (d) between the cation (i) and the anion (iii) in form **II**. Symmetry codes are given in Fig. 2.

of the anions (ii) and (iii). The geometries of the hydrogen bonds are: N(4)···O(3) 3.161(4), H(2N)···O(3) 2.35(3) Å. N(4)–H(2N)···O(3) 145(2)°, and N(4)···O(2) 3.053(3), H(1N)···O(2) 2.21(3) Å, N(4)–H(1N)···O(2) 160(3)°, respectively.

In form **I** all the nitro groups lie nearly in the plane of the benzene ring, the torsion angles around the N–C bonds being O(2)–N(1)–C(2)–C(1) 3(1)°, O(4)–N(2)–C(4)–C(3) 5(1)°, and O(6)–N(3)–C(6)–C(5) −8.9(9)°, while in form **II** the O atoms of the nitro groups at the *o*-positions deviate from the benzene-ring plane, the torsion angles around the N–C bonds being O(2)–N(1)–C(2)–C(1) 37.0(3)° and O(6)–N(3)–C(6)–C(5) 32.3(3)° for the *o*-positions, and O(4)–N(2)–C(4)–C(3) 1.0(4)° for the *p*-position. The C(1)–O(1) lengths in both forms are comparable with those found in some picrate ions.[9,10] In form **I** the bond lengths of O(2)–N(1) and O(3)–N(1) of the nitro group which is free from hydrogen bond are abnormally short because of large thermal vibrations.

Optical Properties of the Form I Crystal. The crystal of the form **I** has four cations (2-iodoanilinium) and four anions (picrate) in the unit cell, as shown in Fig. 2(a) and (b). The polarized IR absorption spectra of the form **I** crystal are shown in Fig. 5. The sharp band at 3082 cm^{-1} can be assigned to the C–H stretching mode of the aromatic rings and three intense peaks in the region from 2400 to 3000 cm^{-1} are assigned to the overlap of the N–H symmetric and antisymmetric stretching modes of the NH_3^+ group and the intense band at 2000 cm^{-1} to the overtones and combinations of the NH_3^+ bending modes.[11] These assignments are in agreement with the results of the X-ray crystal analysis. The polarized visible absorption spectra of the picric acid and the form **I** crystals are shown in Fig. 6. Crystals of picric acid are pale yellow and have the absorption band at 400 nm, but these of 2-iodoaniline are colorless and have no absorption band in the visible region. On the other hand, 2-iodoanilinium picrate crystals are yellow and have the absorption band at 400 nm. That is, no new band between 2-iodoanilinium cation and picrate anion is observed in the visible region, as is expected from the crystal structure (Fig. 2). The locally excited (LE) band of the picrate anion at 400 nm

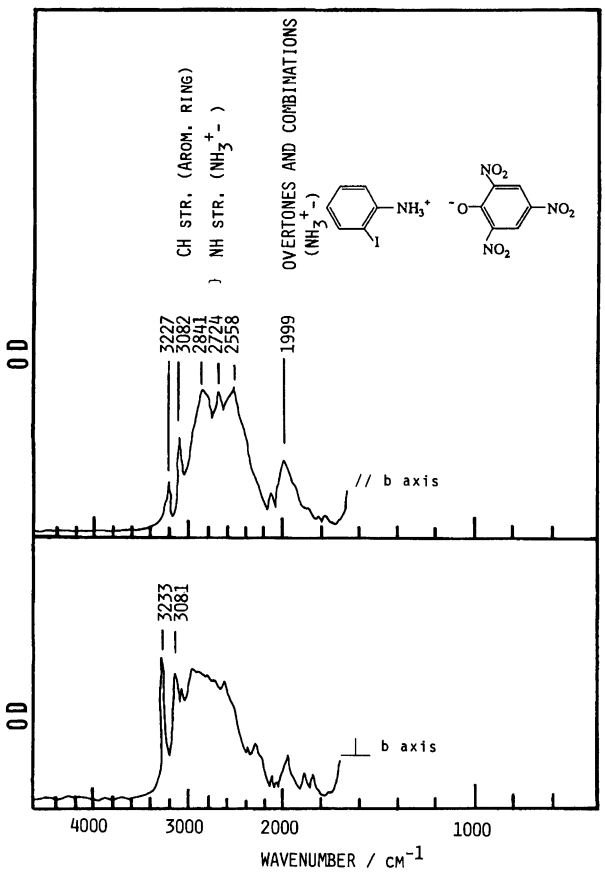

Fig. 5. The polarized IR absorption spectra of the Form **I** crystal.

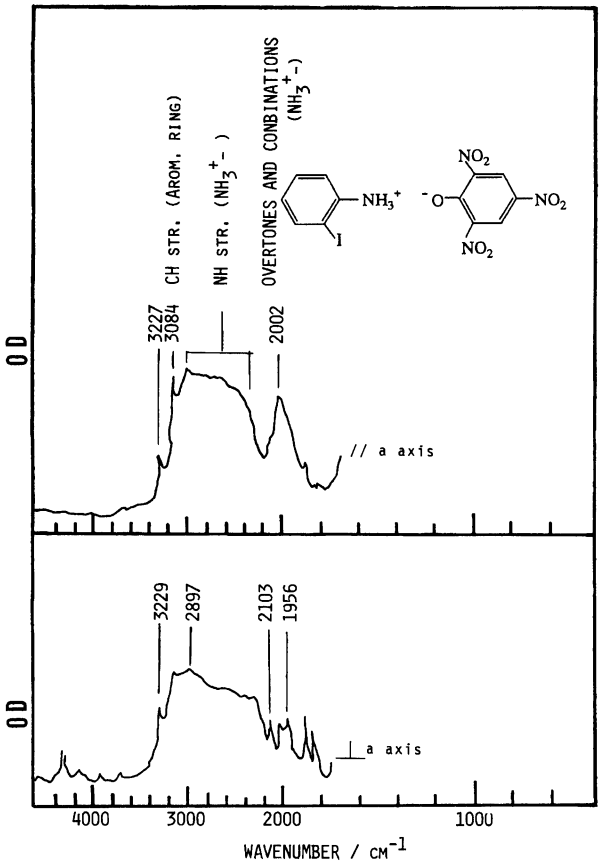

Fig. 7. The polarized IR absorption spectra of the form **II** crystal.

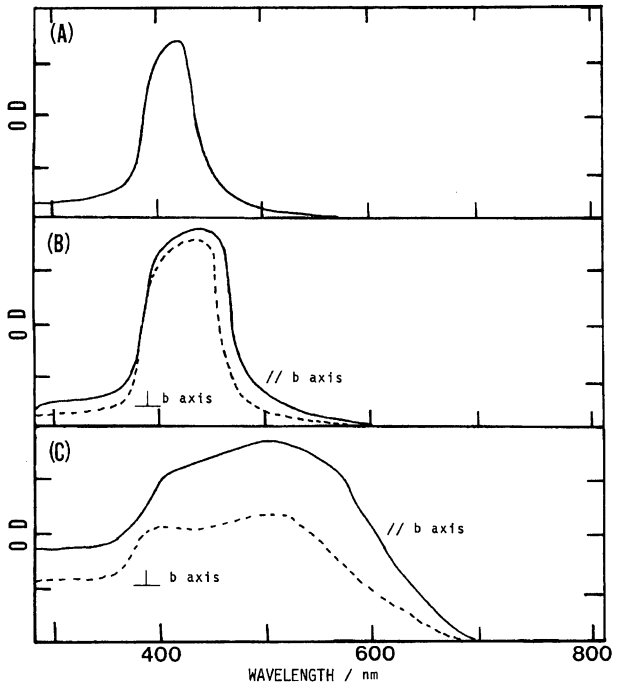

Fig. 6. The polarized visible absorption spectra at room temperature of the picric acid (a) and the form **I** crystals (b: before heating and c: after heating at 60 °C) on the *bc* plane.

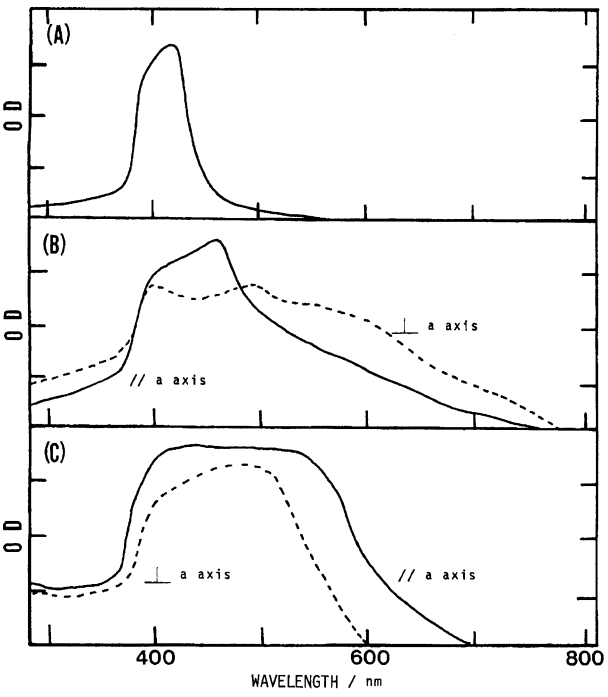

Fig. 8. The polarized visible absorption spectra at room temperature of the picric acid (a) and the form **II** crystals (b: before heating and c: after heating at 60 °C) on the *ac* plane.

has the dichroism of $P(\mathbf{I_b}/\mathbf{I_c})=1.1$ and the direction of the transition moment is parallel to the direction of the pseudo C_2 axis of the picrate anion which is the direction connecting the O(1)–C(1) and C(4)–N(2) bonds.

Optical Properties of the Form II Crystal. The crystal of the form **II** has two cations (2-iodoanilinium) and two anions (picrate) in the unit cell, as shown in Fig. 2(c) and (d). The polarized IR absorption spectra of the form **II** crystal are shown in Fig. 7. Each observed peak can be assigned in the same way as the form **I**. The polarized visible absorption spectra of the picric acid and the form **II** crystals are shown in Fig. 8. 2-Iodoanilinium picrate crystals are dark-green and the broad absorption band occurs over a wide region from 700 to 500 nm in addition to the locally excited (LE) band of picrate anion at 400 nm. The LE band is estimated to have the dichroism of $P(\mathbf{I_a}/\mathbf{I_c}*)=$ca. 0.2 because the direction of the transition moment is in the direction of the O(1)–C(1) and C(4)–N(2) bonds as is mentioned above. However, the observed value is about 0.8. The difference between the observed and calculated values may be explained by the overlap of the broad band which is assigned to the CT band between 2-iodoanilinium cation and picrate anion. This CT band has the peak at about 600 nm for the light polarized perpendicular to the **a** axis and appears as the widebased absorption band in the region from 800 to 500nm for the light polarized parallel to the **a** axis. However, the observed dichroism value $P(\mathbf{I_a}/\mathbf{I_c}*)$ smaller than one means the possibility of mixing the pure CT and LE configurations.

Thermochromism of the Form I and II Crystals. Figure 9 shows the differential scanning calorimatory (DSC) curves of the form **I** and **II** crystals. In the form **I** system, three endothermic peaks (62.8, 92.7 and 118.3 °C) were observed for the DSC curve. The yellow needle crystal of the form **I** complex changed to the red crystal upon being heated at higher temperature than 60 °C. Figure 10 shows the polarized IR spectra of the pyroproduct. The sharp peaks at 3468 and 3374 cm^{-1} is assigned to the N–H stretching mode of the free NH_2 group and the peak at 3106 cm^{-1} to the C–H stretching mode of the aromatic ring. This fact means that the proton transfer reaction occurs upon heating as shown in Fig. 11. The polarized visible absorption spectra of the pyroproduct are shown in Fig. 6. The spectrum polarized parallel to the *b* axis has the peak at 500 nm and the shoulder at 400nm. The spectrum polarized perpendicular to the *b* axis has two peaks at 520 and 400 nm. The 400 nm band is assigned to the LE band of the picric acid. On the other hand, the 520 nm band has the dichromism of $P(\mathbf{I_b}/\mathbf{I_c})=1.7$ and the direction of the transition moment has the component of the direction perpendicular to the molecular planes of picric acid and 2-iodoaniline. Therefore, the band at 520 nm may be assigned to the CT transition band between the picric acid and 2-iodoaniline, and the crystal structure is expected to change from the segregated column system to the mixed stacked column system.

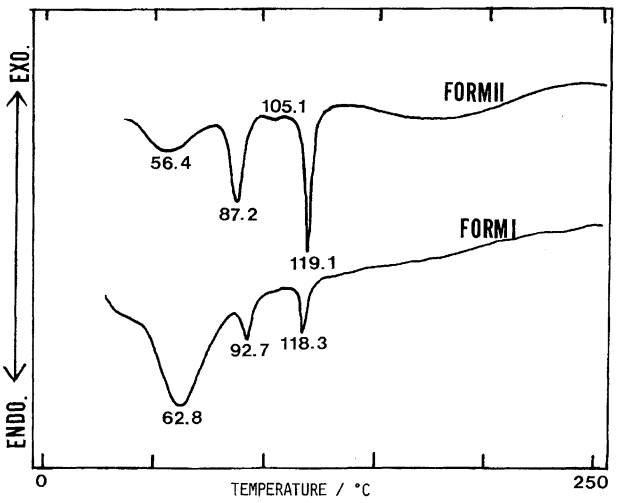

Fig. 9. DSC curves of the forms **I** and **II** crystals of the 2-iodoanilinium picrate complexes.

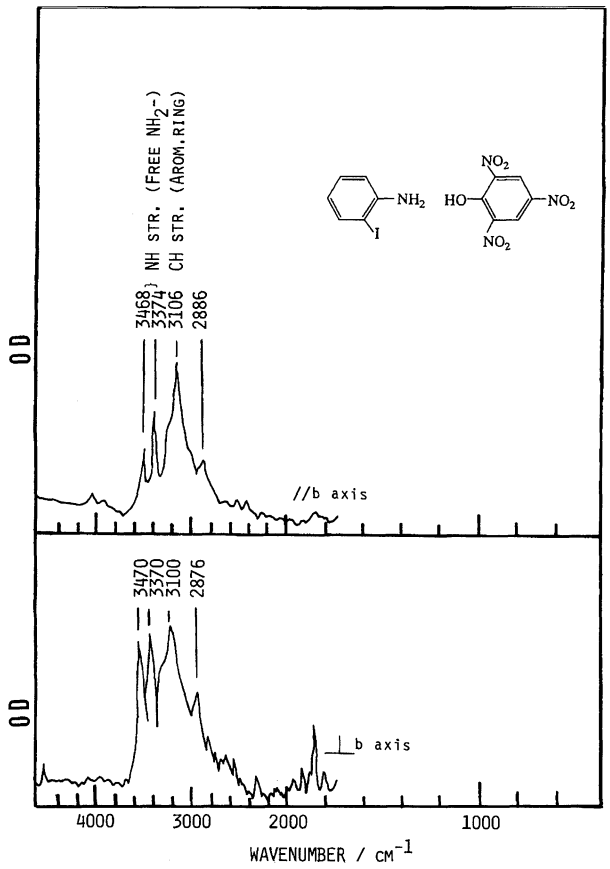

Fig. 10. The polarized IR absorption spectra at room temperature of the pyroproduct of the form **I**.

In the form **II** system, four endopeaks (56.4, 87.2, 105.1, and 119.1 °C) were observed for the DSC curve as is shown in Fig. 9. The dark green plate crystal changed to the red crystal at higher temperature than 60 °C. Figure 12 shows the //*a*-axis IR spectrum of the

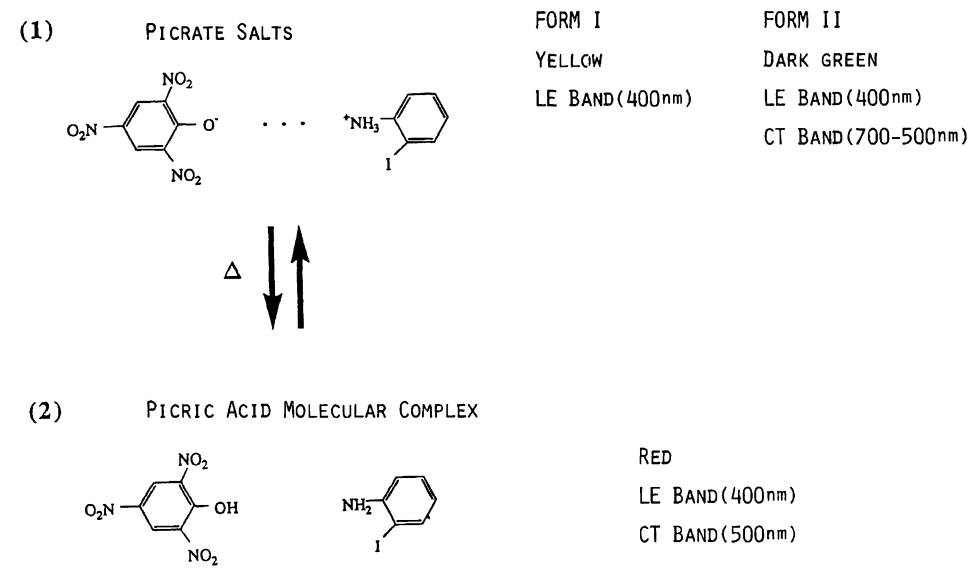

Fig. 11. The mechanism of the thermochromism.

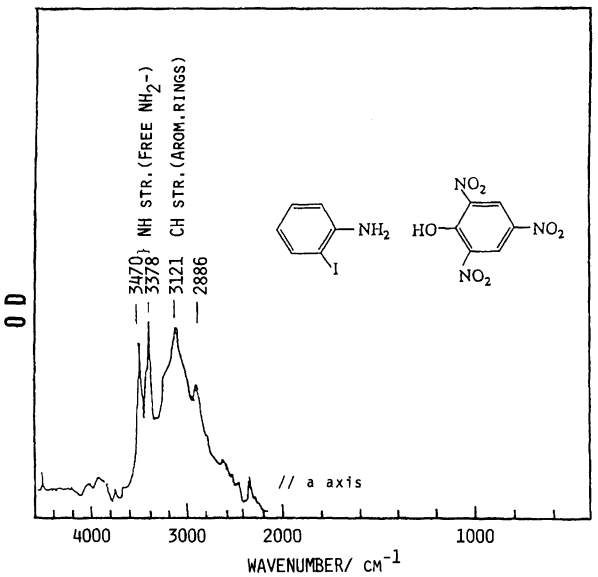

Fig. 12. The polarized IR absorption spectra at room temperature of the pyroproduct of the form **II**.

pyroproduct. The //c^*-axis spectrum has the same behavior as the //a-axis spectrum in the region from 4000 to 2000 cm^{-1}. As well, the spectra look like those of the pyroproduct of the form **I**. That is, the sharp peaks at 3470 and 3378 cm^{-1} are assigned to the N–H stretching mode of the free NH_2 group and the peak at 3121 cm^{-1} to the C–H stretching mode of the aromatic ring. That is, the proton transfer occurs upon heating. The polarized visible absorption spectra shown in Fig. 8(c) are similar to the ones observed in the form **I** system as is expected from the IR spectral change. The 500 nm band is assigned to the CT band and the 400 band to the LE band of the picric acid. Therefore, the mechanism of the thermochromism is shown by the reaction given in Fig. 11.

References

1) G. L. Gartland, G. R. Freeman, and C. E. Bugg, *Acta Crystallogr., Sect. B*, **B30**, 1841 (1974).

2) a) G. Briegleb and H. Delle, *Z. Elektrochem.*, **64**, 347 (1960); b) G. Saito and Y. Matsunaga, *Bull. Chem. Soc. Jpn.*, **44**, 3328 (1971); **46**, 714 (1973); c) E. Hertel, *Ann.*, **451**, 179 (1926); d) E. Hertel and J. van Cleef, *Ber.*, **61**, 1545 (1928).

3) F. H. Herbstein and M. Kaftory, *Acta Crystallogr., Sect. B*, **B31**, 60 (1975).

4) M. Tanaka, "The 4-th Jikken Kagakukouza," ed by K. Yoshihara, Maruzen, Tokyo (1992), Vol. 4, No. 7, Bunkou II, p. 314.

5) G. J. Gilmore, *J. Appl. Crystallogr.*, **17**, 42 (1984).

6) "International Tables for X-Ray Crystallogrphy," Kynoch Press, Birmingham (Present distributor Kluwer Academic Publisher, Dordrecht) (1974), Vol. IV, pp. 22—98.

7) "TEXAN. Single Crystal Structure Analysis Software, Version 5.0," Molecular Corporation, The Woodlands, Texas (1989).

8) Tables of anisotropic thermal parameters, atomic parameters of hydrogen atoms, bond lengths and angles involving hydrogen atoms, and structure factors have been deposited on Document No. 67034 at the Office of the Editor of Bull. Chem. Soc. Jpn.

9) C. L. Jones, G. H. Milburn, L. Sawyer, and D. L. Hughes, *Acta Crystallogr., Sect. B*, **37**, 1548 (1981).

10) G. Ferguson, B. L. Ruhl, T. Wieckowski, D. Lloyed, and H. McNab, *Acta Crystallogr., Sect. C*, **40**, 1740 (1984).

11) R. Newman and R. S. Halford, *J. Chem. Phys.*, **18**, 1276 (1950).